Molecular Orbital and IMOMM Studies of the Chain Transfer Mechanisms of the Diimine−M(II)-Catalyzed (M = Ni, Pd) Ethylene Polymerization Reaction

Djamaladdin G. Musaev,* Robert D. J. Froese, and Keiji Morokuma*

Cherry L. Emerson Center for Scientific Computation and Department of Chemistry, Emory University, Atlanta, Georgia 30322

Received December 16, 1997

Associative displacement and H-exchange chain transfer/termination mechanisms for the diimine−M(II)-catalyzed (M = Ni, Pd) ethylene polymerization have been studied using B3LYP and IMOMM methods. For unsubstituted diimine complexes the coordination of ethylene to the metal−olefin−hydride complexes $L_2M(C_2H_4)H^+$ and $L_2M(C_3H_6)H^+$ is exothermic and gives the five-coordinate complex **22**. From **22**, the following processes can take place: (a) the associative displacement, path **E**, corresponding to dissociation of propylene, (b) the dissociation of ethylene, reverse path **D**, (c) the H-exchange, path **F**, and (d) the reattaching of the hydrogen to the polymer chain, path **G**. For M = Ni, the associative displacement cannot compete with paths **F** and **G** and is unlikely to take place. For M = Pd, the energetics for the paths **E**−**G** are similar, and the chain transfer/termination via the associative dissociation path **E** is more likely. The H-exchange process, path **F**, is the most favorable chain transfer/termination mechanism for both metals and includes (a) oxidative addition of the β-agostic $C^{\beta}-H^{agostic}$ bond to the metal center to form the metal−olefin−hydride complex **21**, (b) the coordination of ethylene to the metal center to form the five-coordinate complex **22**, and (c) migration of the hydrogen atom from the metal to the ethylene molecule. The rate-determining steps are steps a and c for the diimine−Ni- and diimine−Pd-catalyzed reactions, respectively. The substitution of the imine hydrogens with bulky aromatic groups 2,6-$C_6H_3(i\text{-Pr})_2$ makes **22** thermodynamically unstable relative to C_2H_4 + diimine-$M(C_3H_7)^+$. Therefore, all processes starting from **22** become unimportant. These results were compared with the previously studied β-hydrogen transfer and hydrogenolysis chain transfer mechanisms.

I. Introduction

During the past few decades, the mechanism of transition-metal-catalyzed olefin polymerization reactions has been a focus of extensive studies.[1−9] In general, these studies can be divided into two distinct classes. The first of these deals with the study and adjustment of the ligand, cocatalyst, solvent, and metal in an effort to improve the catalytic activity of the existing technology. The second is the search for new and more active alternative catalysts. This paper is a continuation of our previous studies[4−8] on the mechanisms of the relatively new diimine−M(II)-catalyzed ethylene polymerization reactions. Previously,[4−7] we have studied in detail, as shown in Scheme 1, the mechanism of the reactions

chain initiation:

$$[L_2MCH_3]^+ + C_2H_4 \rightarrow [L_2MCH_2CH_2CH_3]^+ \quad (1)$$

two chain propagation steps:

$$[L_2MCH_2CH_2CH_3]^+ + C_2H_4 \rightarrow [L_2M(CH_2CH_2)_2CH_3]^+ \quad \text{path } \mathbf{A} \quad (2)$$

$$[L_2MCH_2CH_2CH_3]^+ \rightarrow [L_2M(H)(CH_2{=}CHCH_3)]^+ \rightarrow [L_2MCH(CH_3)_2]^+ + C_2H_4$$

$$\rightarrow [L_2MCH_2CH_2CH(CH_3)_2]^+ \quad \text{path } \mathbf{B} \quad (3)$$

These lead to linear and methyl-branched polyethylenes, respectively.

(1) As leading references, see: (a) Huang, J.; Rempel, G. L. *Prog. Polym. Sci.* **1995**, *20*, 459 and references therein. (b) Coates, G. W.; Waymouth, R. M. *Science* **1995**, *267*, 217. (c) van der Linden, A.; Schaverien, C. J.; Meijboom, N.; Ganter, C.; Orpen, A. G. *J. Am. Chem. Soc.* **1995**, *117*, 3008. (d) Yang, X.; Stern, C. L.; Marks, T. J. *J. Am. Chem. Soc.* **1994**, *116*, 10015. (e) Coughlin, E. B.; Bercaw, J. E. *J. Am. Chem. Soc.* **1992**, *114*, 7606. (f) Crowther, D. J.; Baenziger, N. C.; Jordan, R. F. *J. Am. Chem. Soc.* **1991**, *113*, 1455. (g) Kaminsky, W.; Kulper, K.; Brintzinger, H. H.; Wild, F. R. W. P. *Angew. Chem., Int. Ed. Engl.* **1985**, *24*, 507. (h) Ewen, J. A. *J. Am. Chem. Soc.* **1984**, *106*, 6355. (i) Alameddin, N. G.; Ryan, M. F.; Eyler, J. R.; Siedle, A. R.; Richardson, D. E. *Organometallics* **1995**, *14*, 5005 and references therein.

(2) As leading references, see: (a) Yoshida, T.; Koga, N.; Morokuma, K. *Organometallics* **1995**, *14*, 746. (b) Yoshida, T.; Koga, N.; Morokuma, K. *Organometallics* **1996**, *15*, 766. (c) Woo, T. K.; Fan, L.; Ziegler, T. *Organometallics* **1994**, *13*, 2252. (d) Weiss, H.; Ehrig, M.; Ahlrichs, R. *J. Am. Chem. Soc.* **1994**, *116*, 4919. (e) Fan, L.; Harrison, D.; Woo, T. K.; Ziegler, T. *Organometallics* **1995**, *14*, 2018. (f) Lohrenz, J. C. W.; Woo, T. K.; Ziegler, T. *J. Am. Chem. Soc.* **1995**, *117*, 12793. (g) Hyla-Kryspin, I.; Niu, S.; Gleiter, R. *Organometallics* **1995**, *14*, 964. (h) Fan, L.; Harrison, D.; Deng, L.; Woo, T. K.; Swerhone, D.; Ziegler, T. *Can. J. Chem.* **1995**, *73*, 989. (i). Lohrenz, J. C. W.; Woo, T. K.; Fan, L.; Ziegler, T. *J. Organomet. Chem.* **1995**, *497*, 91.

S0276-7333(97)01103-5 CCC: $15.00
Publication on Web 04/04/1998

Scheme 1. Proposed Mechanism of the Diimine−M(II)-Catalyzed Ethylene Polymerization Reaction[a]

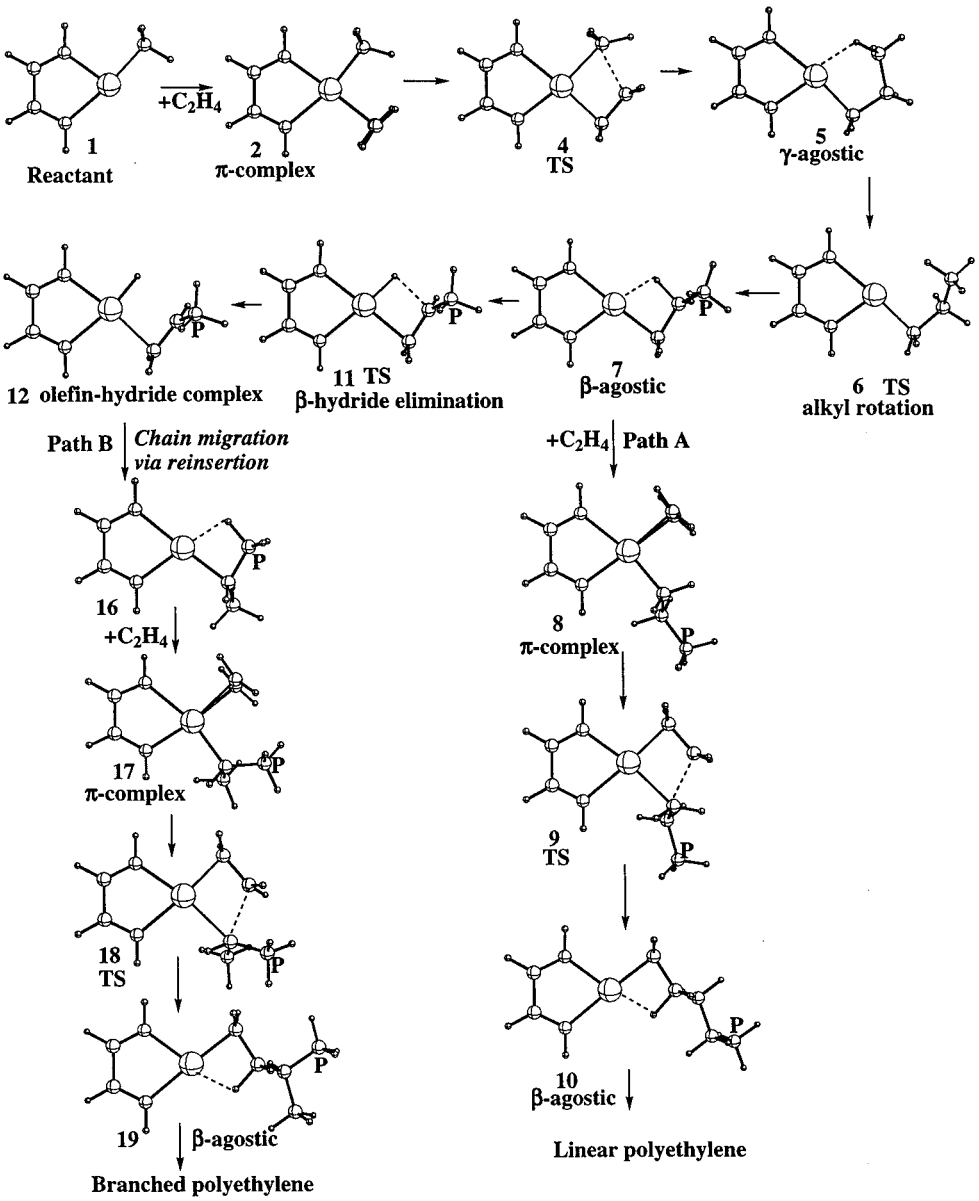

[a] The methyl group labeled "P" is the polymer chain in the polymerization process.

chain-termination (dissociative displacement or β-H elimination followed by olefin dissociation):

$$[L_2MCH_2CH_2CH_3]^+ \rightarrow [L_2M(H)(CH_2{=}CHCH_3)]^+ \rightarrow [L_2MH]^+ + CH_2{=}CHCH_3 \quad (4)$$

chain termination (hydrogenolysis):

$$[L_2MCH_2CH_2CH_3]^+ + H_2 \rightarrow [L_2M(H_2)CH_2CH_2CH_3]^+ \rightarrow [L_2MH]^+ + CH_3CH_2CH_3 \quad (5)$$

for M = Ni and Pd and L_2 = [HN=C(H)C(H)=NH][4−6] and [ArN=C(H)C(H)=NAr],[7] where Ar = 2,6-C_6H_3(*i*-Pr)$_2$.

In the current paper our goal is to study two additional chain transfer/termination processes:

H-exchange between alkyl and olefin fragments:

$$[L_2M(C_2H_4)(RH)]^+ \rightarrow [L_2M(C_2H_5)R]^+ \quad (6)$$

RH = *n*-C_3H_7 and *i*-C_3H_7

associative displacement:

$$[L_2M(H)(CH_2{=}CH_2)]^+ + C'H_2{=}C'H_2 \rightarrow [L_2M(H)(CH_2{=}CH_2)(C'H_2{=}C'H_2)]^+ \rightarrow [L_2M(H)(C'H_2{=}C'H_2)]^+ + CH_2{=}CH_2 \quad (7)$$

where the coordinating olefin is rapidly exchanged with ethylene from solution. The existence of a five-coordinate bis(olefin) complex is essential to this process. We have discussed briefly an H-exchange mechanism in earlier papers for the diimine−Pd-catalyzed process.[4−6]

(3) (a) Johnson, L. K.; Killian, C. M.; Brookhart, M. *J. Am. Chem. Soc.* **1995**, *117*, 6414. (b) Johnson, L. K.; Mecking, S.; Brookhart, M. *J. Am. Chem. Soc.* **1996**, *118*, 267.

(4) Musaev, D. G.; Froese, R. D. J.; Svensson, M.; Morokuma, K. *J. Am. Chem. Soc.* **1997**, *119*, 367.

(5) Musaev, D. G.; Svensson, M.; Morokuma, K.; Stromberg, S.; Zetterberg, K.; Siegbahn, P. E. M. *Organometallics* **1997**, *16*, 1933.

(6) Musaev, D. G.; Froese, R. D. J.; Morokuma, K. *New J. Chem.* **1997**, *21*, 1269.

However, those results were not enough to draw final conclusions. Therefore, we have decided to reinvestigate it in more detail for both the diimine−Ni and −Pd catalysts in the present paper.

In part II, the methods of computation are described. In part III, we will discuss the processes starting from the five-coordinate bis(olefin)−metal−hydride complex, while in part IV we will compare the mechanisms of different chain transfer/termination processes. In part V a comparison of our previous and present results with those of a related study by Ziegler and co-workers[9] will be given. In part VI, we will summarize the results and give conclusions.

II. Calculation Procedure

Geometries and energies of the reactants, intermediates, transition states, and products of the reactions are calculated using the hybrid density functional theory B3LYP,[10] which has been shown to predict quite reliable geometries and energies.[11] We consider only the closed-shell singlet, as the triplet state is expected to be higher in energy for all the structures studied. In these calculations we used basis set I (below denoted as BSI) which includes the standard lanl2dz basis set (8s5p5d)/[3s3p2d] and (8s6p4d)/[3s3p2d] with the ECP (relativistic for Pd) developed by Hay and Wadt[12] replacing core electrons up to 2p and 3d for Ni and Pd, respectively, and the valence double-ζ basis set of Huzinaga and Dunning[13] for the active part, i.e., the C and H atoms of alkyl groups and olefins. The standard 3-21G basis set[14] was adopted for the N, C, and H atoms of the ligand L_2 = [HN═C(H)C(H)═NH]. As shown in a previous paper for M = Pd,[5] BSI describes the geometries and energetics quite well. All structures were optimized without symmetry constraints. Normal-mode analysis has been performed for most of the structures, and zero-point energy correction (ZPE) and entropy effects (such the Gibbs free energy) are included in some of our final energetics. All calculations have been performed by a modified Gaussian-94 package.[15,16]

We have also performed a series of calculations for the $L_2Ni(C_2H_5)(C_2H_4)^+$ complex at the B3LYP and BP86 levels using a large all-electron basis set (below denoted as BSII) including the (14s11p5d)/[8s6p2d] basis set of Wachters[17] augmented with diffuse[18] d and polarization[19] f functions for Ni, the triple-ζ 6-311G(d,p)[20e,f] set for the active C and H atoms, and the 6-31G(d,p)[20a−d] set for diimine.

To elucidate the role of the substitution in the diimine ligand, we have also studied several paths and structures for L'_2 = [ArN═C(H)C(H)═NAr], where Ar = 2,6-$C_6H_3(i\text{-}Pr)_2$, at the IMOMM level. In this integrated method,[21] the energy of the system of interest, the "real system", is represented by a sum of the MO energy of a smaller "model system" and the MM energy (excluding the part taken into account in the MO energy, to avoid double counting) of the "real system". In the present calculation, all the active atoms, the incoming olefins, the M−R (R = H and CH_3) fragment, and the unsubstituted diimine [HN═C(H)C(H)═NH] ligand, were included in the model system, which has been treated by the pure MO method. The real system contains the full diimine [ArN═C(R)C(R)═NAr], where Ar = 2,6-$C_6H_3(i\text{-}Pr)_2$ and R = Me, in place of the unsubstituted diimine in the model system. For the MO part, the B3LYP/BSI method was used. For the MM part, the MM3 force field[22] without the electrostatic contribution was used. The van der Waals parameters reported by Rappe et al. are used for the metal atoms,[23] while all torsional contributions associated with dihedral angles involving metal atoms are set to zero. Other MM contributions involving the metal are set to zero in the IMOMM method, and no additional parameters are used. Adopting R = H and Ar = H as the common model system, we have fixed the N−H and C−H (set 2) bond lengths at the optimized values for pure MO calculations for the model system and the N−C(Ar) and

(7) Froese, R. D. J.; Musaev, D. G.; Morokuma, K. *J. Am. Chem. Soc.* **1998**, *120*, 1581.
(8) Froese, R. D. J.; Musaev, D. G.; Matsubara, T.; Morokuma, K. *J. Am. Chem. Soc.* **1997**, *119*, 7190.
(9) (a) Deng, L.; Margl, P.; Ziegler, T. *J. Am. Chem. Soc.* **1997**, *119*, 1094. (b) Deng, L.; Woo, T. K.; Cavallo, L.; Margl, P.; Ziegler, T. *J. Am. Chem. Soc.* **1997**, *119*, 6177.
(10) (a) Becke, A. D. *Phys. Rev. A* **1988**, *38*, 3098. (b) Lee, C.; Yang, W.; Parr, R. G. *Phys. Rev. B* **1988**, *37*, 785. (c) Becke, A. D. *J. Chem. Phys.* **1993**, *98*, 5648.
(11) (a) Musaev, D. G.; Morokuma, K. *J. Phys. Chem.* **1996**, *100*, 6509. (b) Erikson, L. A.; Pettersson, L. G. M.; Siegbahn, P. E. M.; Wahlgren, U. *J. Chem. Phys.* **1995**, *102*, 872. (c) Ricca, A.; Bauschlicher, C. W., Jr. *J. Phys. Chem.* **1994**, *98*, 12899. (d) Heinemann, C.; Hertwig, R. H.; Wesendrup, R.; Koch, W.; Schwarz, H. *J. Am. Chem. Soc.* **1995**, *117*, 495. (e) Hertwig, R. H.; Hrusak, J.; Schroder, D.; Koch, W.; Schwarz, H. *Chem. Phys. Lett.* **1995**, *236*, 194. (f) Schroder, D.; Hrusak, J.; Hertwig, R. H.; Koch, W.; Schwerdtfeger, P.; Schwarz, H. *Organometallics* **1995**, *14*, 312. (g) Fiedler, A.; Schroder, D.; Shaik, S.; Schwarz, H. *J. Am. Chem. Soc.* **1994**, *116*, 10734. (h) Fan, L.; Ziegler, T. *J. Chem. Phys.* **1991**, *95*, 7401. (i) Berces, A.; Ziegler, T.; Fan, L. *J. Phys. Chem.* **1994**, *98*, 1584. (j) Lyne, P. D.; Mingos, D. M. P.; Ziegler, T.; Downs, A. J. *Inorg. Chem.* **1993**, *32*, 4785. (k) Li, J.; Schreckenbach, G.; Ziegler, T. *J. Am. Chem. Soc.* **1995**, *117*, 486. (l) Bernardi, F.; Bottoni, A.; Calcinari, M.; Rossi, I.; Robb, M. A. *J. Phys. Chem. A* **1997**, *101*, 6310.
(12) (a) Hay, P. J.; Wadt, W. R. *J. Chem. Phys.* **1985**, *82*, 299. (b) Wadt, W. R.; Hay, P. J. *J. Chem. Phys.* **1985**, *82*, 284.
(13) (a) Dunning, T. M., Jr. *J. Chem. Phys.* **1971**, *55*, 716. (b) Dunning, T. M., Jr. *J. Chem. Phys.* **1970**, *53*, 2823.
(14) Binkley, J. S.; Pople, J. A.; Hehre, W. J. Self-Consistent Molecular Orbital Methods. 21. *J. Am. Chem. Soc.* **1980**, *102*, 939.
(15) Frisch, M. J.; Trucks, G. W.; Schlegel, H. B.; Gill, P. M. W.; Johnson, B. G.; Robb, M. A.; Cheesemen, J. R.; Keith, T. A.; Petersson, J. A.; Montgomery, J. A.; Raghavachari, K.; Al-Laham, M. A.; Zakrzewski, V. G.; Ortiz, J. V.; Foresman, J. B.; Cioslowski, J.; Stefanov, B. B.; Nanayakkara, A.; Challacombe, M.; Peng, C. Y.; Ayala, P. Y.; Chen, W.; Wong, M. W.; Andres, J. L.; Replogle, E. S.; Gomperts, R.; Martin, R. L.; Fox, D. J.; Binkley, J. S.; DeFrees, D. J.; Baker, J.; Stewart, J. J. P.; Head-Gordon, M.; Gonzales, C.; Pople, J. A. Gaussian 94; Gaussian Inc., Pittsburgh, PA, 1995.
(16) Cui, Q.; Musaev, D. G.; Svensson, M.; Morokuma, K. *J. Phys. Chem.* **1996**, *100*, 10936.
(17) Wachters, A. J. H. *J. Chem. Phys.* **1970**, *52*, 1033.
(18) Hay, P. J. *J. Chem. Phys.* **1977**, *66*, 4377.
(19) Bauschlicher, C. W., Jr.; Walch, S. P.; Partridge, H. *J. Chem. Phys.* **1982**, *76*, 1033.
(20) (a) Ditchfield, R.; Hehre, W. J.; Pople, J. A. *J. Chem. Phys.* **1971**, *54*, 724. (b) Hehre, W. J.; Ditchfield, R.; Pople, J. A. *J. Chem. Phys.* **1972**, *56*, 2257. (c) Hariharan, P. C.; Pople, J. A. *Mol. Phys.* **1974**, *27*, 209. (d) Gordon, M. S. *Chem. Phys. Lett.* **1980**, *76*, 163. (e) McLean, A. D.; Chandler, G. S. *J. Chem. Phys.* **1980**, *72*, 5639. (f) Krishnan, R.; Binkley, J. S.; Seeger, R.; Pople, J. A. *J. Chem. Phys.* **1980**, *72*, 650.
(21) (a) Maseras, F.; Morokuma, K. *J. Comput. Chem.* **1995**, *16*, 1170. (b) Matsubara, T.; Maseras, F.; Koga, N.; Morokuma, K. *J. Phys. Chem.* **1996**, *100*, 2573. (c) Matsubara, T.; Sieber, S.; Morokuma, K. *Int. J. Quantum Chem.* **1996**, *60*, 1101. (d) Froese, R. D. J.; Morokuma, K. *Chem. Phys. Lett.* **1996**, *263*, 393.
(22) (a) MM3(92): Quantum Chemistry Program Exchange, Indiana University, 1992. (b) Aped, A.; Allinger, N. L. *J. Am. Chem. Soc.* **1992**, *114*, 1.
(23) Rappe, A. K.; Casewit, C. J.; Colwell, K. S.; Goddard, W. A., III; Skiff, W. M. *J. Am. Chem. Soc.* **1992**, *114*, 10024.
(24) Frisch, M. J.; Trucks, G. W.; Schlegel, H. B.; Gill, P. M. W.; Johnson, B. G.; Wong, M. W.; Foresman, J. B.; Robb, M. A.; Head-Gordon, M.; Replogle, E. S.; Gomperts, R.; Andres, J. L.; Raghavachari, K.; Binkley, J. S.; Gonzales, C.; Martin, R. L.; Fox, D. J.; DeFrees, D. J.; Baker, J.; Stewart, J. J. P.; Pople, J. A. Gaussian 92/DFT; Gaussian Inc., Pittsburgh, PA, 1993.

C−C(Me) (set 3) bond lengths at 1.45 and 1.51 Å, respectively. Calculations were performed using our own IMOMM program,[21] which contains modified MM3-(92)[22] and modified Gaussian-92/DFT programs.[24] All structures were optimized without symmetry constraints.

III. Various Reactions of Metal−Olefin−Hydride Complex 21

Scheme 1 shows intermediates, transition states, and products of the polymer initiation (reaction 1) and the chain propagation reactions (eqs 2 and 3) leading to linear and methyl-branched polyethylene, respectively (structures **1**−**19**), which were discussed in more detail in our previous papers.[4−6] Analysis of the reactions (4), (6), and (7) shows that the starting structure for these is the same metal−olefin−hydride complex.

Therefore, at first let us discuss the structure and stabilities of the metal−olefin−hydride complex **21** (**12** in Scheme 1). As seen from Figure 1 and Table 1, the coordination of ethylene and propylene to the L_2MH^+ complex **20** forms stable π-complexes, $L_2M(C_2H_4)H^+$ (**21a**) and $L_2M(C_3H_6)H^+$ (**21b**), respectively, with the C═C bond positioned (approximately for **21b**) perpendicular to the M(N═CC═N) plane. (Note that **a** and **b** stand for complexes of ethylene and propylene, respectively.) Both of these complexes are confirmed to be real minima by the normal-mode analysis and are separated with a small energy barrier, leading to the energetically most stable β-agostic $L_2M(C_2H_5)^+$ and $L_2M(C_3H_7)^+$ complexes (structures not shown here),[4−6] respectively. The energy differences between the π-complexes $L_2M(C_2H_4)H^+$ (**21a**) and $L_2M(C_3H_6)H^+$ (**21b**) and their respective β-agostic complexes $L_2M(C_2H_5)^+$ and $L_2M(C_3H_7)^+$ are, as seen in Table 1, 18.4 [9.5] and 13.6 [5.4] kcal/mol for M = Ni (values for M = Pd are given in brackets throughout the rest of this paper). The complexation energies of olefin for **21a** and **21b** are respectively 35.9 [38.1] and 40.3 [41.9] kcal/mol. For $L_2M(C_2H_4)H^+$ (**21a**), the inclusion of ZPE reduces these values by 1.5−2.0 kcal/mol, and the entropy effect makes the Gibbs free energies (at 298 K and 1 atm) to be 24.1 [26.0] kcal/mol. Comparison of the values between the corresponding ethylene and propylene complexes shows that propylene binds to the metal center a few kcal/mol more strongly than ethylene, which should be the result of the difference in electron-donating capabilities between CH_3 and H. We should note that, as shown in our previous papers,[4,5,6] the olefin−metal−hydride complex can easily (with a barrier of a few kcal/mol) rearrange to the metal−alkyl complex.

Next, we will examine several possible processes starting from complex **21**, which are summarized in Scheme 2. The first of these is path **B** (reaction 3), leading to methyl-branched polyethylene. The second is path **C**, the dissociative displacement chain transfer/termination mechanism (reaction 4). These two processes have been discussed in detail in our previous papers[4−7] and will not be repeated here. The third, path **D**, is the coordination of the next ethylene molecule to the olefin−metal−hydride complex **21** to form the five-coordinate bis(olefin)−metal−hydride complex **22**. Here our discussions will be concentrated mainly on path **D** and the processes starting from the resultant bis-(olefin)−metal−hydride complex **22**. At first, we would like to note that Ziegler and co-workers are the first who have demonstrated[25] the possible existence of a five-coordinate species in their studies of ethylene oligomerization by (acac)NiH. They also discussed the possible chain termination process via five-coordinate complexes in their latest paper[9] on the diimine−Ni(II)-catalyzed ethylene polymerization reaction (see section V for more details).

Path D. Coordination of a second ethylene molecule to $L_2M(C_2H_4)H^+$ (**21a**) and $L_2M(C_3H_6)H^+$ (**21b**) is downhill and leads respectively to the stable five-coordinate bis(olefin)−metal-hydride complexes $L_2M(C_2H_4)_2H^+$ (**22a**) and $L_2M(C_3H_6)(C_2H_4)H^+$ (**22b**). These bis(olefin)−metal−hydride complexes may have several isomers with the olefins parallel and perpendicular to the M−H bond. For the $L_2M(C_2H_4)_2H^+$ complex, we have found only two of them, structures **22a-1** and **22a-2**, as shown in Figure 1. In **22a-1**, the ethylene molecules are equivalent and, roughly speaking, are placed on a plane perpendicular to the M−H bond and the MNCCN plane. In **22a-2**, one of the ethylene molecules is parallel and the other is perpendicular to the M−H bond and the MNCCN plane. Both of these structures are confirmed to be real minima, among which, as shown in Table 1, **22a-1** is slightly more favorable, by 1.9 [2.1] kcal/mol for M = Ni [Pd]. Another structure with both ethylenes positioned parallel to M−H and MNCCN is expected to be about 4 kcal/mol higher than **22a-1** and was not calculated**.** For $L_2M(C_3H_6)(C_2H_4)H^+$, even more isomers are possible. Since all these isomers are expected to have very similar energies, we have calculated only structure **22b**, with both ethylene and propylene perpendicular. The calculated coordination energies of the ethylene molecule to $L_2M(C_2H_4)H^+$ (**22a-1**) and $L_2M(C_3H_6)H^+$ (**22b**) are 10.3 [6.3] and 7.8 [4.3] kcal/mol. However, the Gibbs free energy at 298 K indicates that this complex formation is slightly endothermic, with negative binding free energies of −2.9 [−5.8] kcal/mol for complex **22a-1**.

The five-coordinate bis(olefin)−metal−hydride complex **22** is the key intermediate for varieties of paths of the polymerization process, as shown in Scheme 2. We will examine these paths in detail.

Path E. This path, the associative displacement chain transfer/termination mechanism, corresponds to the dissociation of propylene (or in reality the olefinic polymer chain) leading to the termination of the polymer growth with the production of an α-olefinic polymer or oligomer and metal−hydride complex, from which a new chain can be started. Table 1 shows that the dissociation of propylene from $L_2M(C_3H_6)(C_2H_4)H^+$ (**22b**) is 12.2 [8.1] kcal/mol endothermic in energy but is slightly (1 and 4 kcal/mol) exothermic for the Gibbs free energy. These values indicate that, from $L_2M(C_3H_6)(C_2H_4)H^+$ (**22b**), ethylene dissociation is more favorable than propylene dissociation by 4.4 [3.8] kcal/mol.

Path F. This path is what is called the H-exchange path and corresponds to the insertion of the new ethylene molecule into the metal−hydride bond to form

(25) (a) Fan, L.; Krzywicki, A.; Somogyvari, A.; Ziegler, T. *Inorg. Chem.* **1996**, *35*, 4003. (b) Fan, L.; Krzywicki, A.; Somogyvari, A.; Ziegler, T. *Stud. Surf. Sci. Catal.* **1996**, *100*, 507.

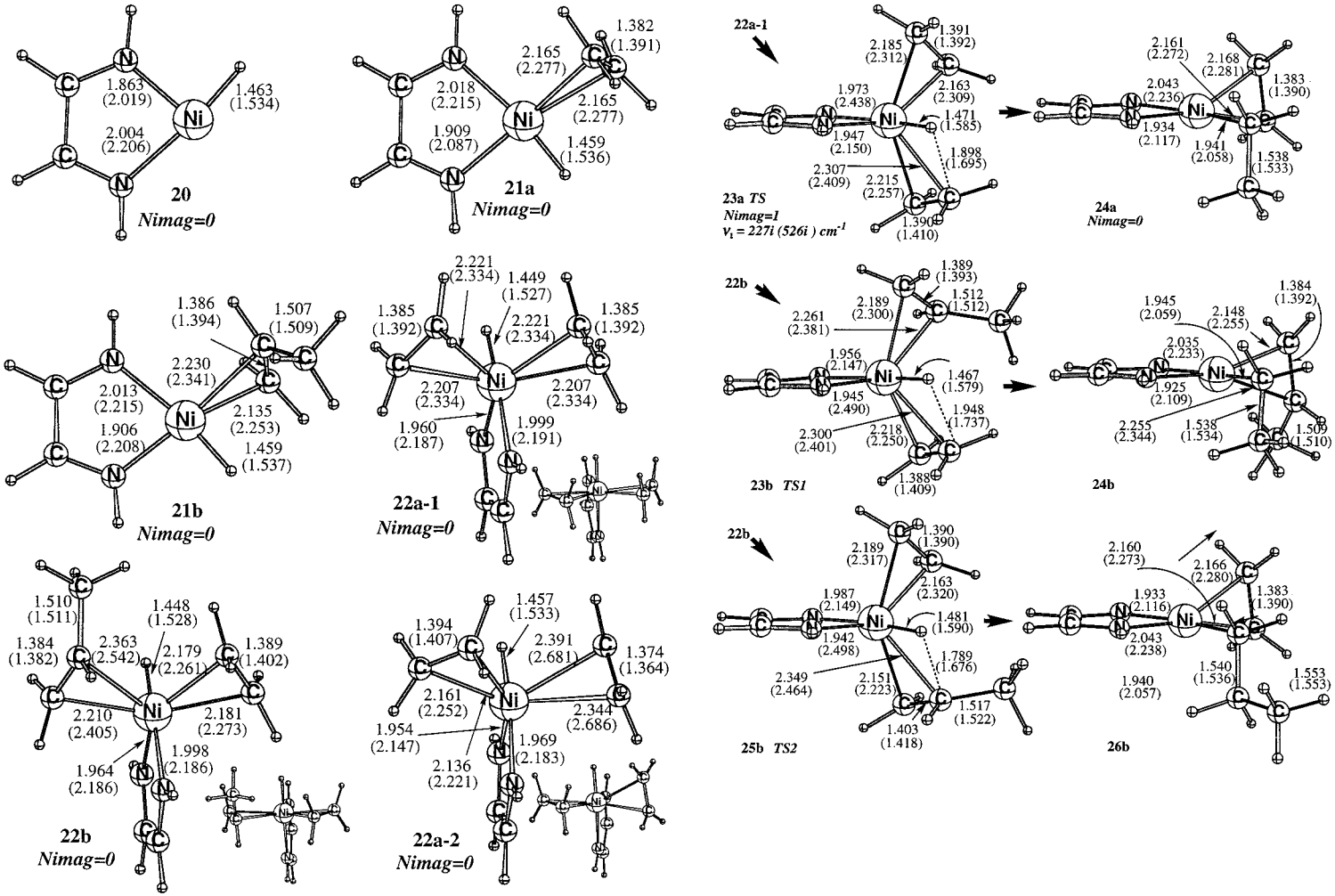

Figure 1. B3LYP/BSI optimized structures (bond distances in Å) of the reactants, transition states, intermediates, and products of reactions 6 and 7 for M = Ni and Pd (in parentheses) and L_2 = [HN=C(H)C(H)=NH]. Nimag is the number of imaginary frequencies, and for Nimag = 1, the actual frequency is shown.

Table 1. Total Energies (in Italics, in Hartrees) of the Reactants and Relative Energies (in kcal/mol) and Gibbs Free Energies (in Parentheses, in kcal/mol at 298 K and 1 atm) of Intermediates and Transition States of the Reactions 6 and 7 for M = Ni and Pd, Calculated at the B3LYP/BSI Level for L_2 = [HN=C(H)C(H)=NH] Systems and at the IMOMM(B3LYP/BSI:MM3) Level for L'_2 = [ArN=C(H)C(H)=NAr] (Ar = 2,6-C_6H_3(*i*-Pr)$_2$) Systems

system	compd no.	M = Ni	M = Pd
C_2H_4		−78.578 208	
C_3H_6		−117.888 548	
L_2MH^+	**20**	−356.724 179	−314.163 115
Reaction of $L_2MH^+ + 2C_2H_4$			
$L_2MH^+ + 2(C_2H_4)$		0.0 (0.0)	0.0 (0.0)
$L_2MH(C_2H_4)^+ + C_2H_4$	**21a**	−35.9 (−24.1)	−38.1 (−26.0)
$L_2MH(C_2H_4)_2^+$	**22a-1**	−46.2 (−21.2)	−44.4 (−20.2)
	22a-2	−44.3	−42.3 (−19.6)
TS	**23a**	−44.0 (−20.0)	−37.1 (−14.5)
$L_2M(C_2H_5)(C_2H_4)^+$	**24a**	−67.1	−66.9
$L_2M(C_2H_5)^+ + C_2H_4$		−54.3	−47.6
Reaction of $L_2MH^+ + C_2H_4 + C_3H_6$			
$L_2MH^+ + C_2H_4 + C_3H_6$		0.0	0.0
$L_2MH(C_3H_6)^+ + C_2H_4$	**21b**	−40.3	−41.9
$L_2MH(C_3H_6)(C_2H_4)^+$	**22b**	−48.1	−46.2
TS1	**23b**	−45.8	−38.8
$L_2M(C_2H_5)(C_3H_6)^+$	**24b**	−70.5	−69.9
TS2	**25b**	−45.9	−38.6
$L_2M(C_3H_7)(C_2H_4)^+$	**26b**	−65.5	−65.3
$L_2M(C_3H_7)^+ + C_2H_4$		−53.9	−47.3
Reaction of $L'_2MH^+ + 2C_2H_4$			
L_2MH^+	**27**	−356.722 514	−314.160 724
$L_2MH^+ + 2C_2H_4$		0.0 [46.4][a]	0.0 [47.1]
$L_2MH(C_2H_4)^+ + C_2H_4$	**28**	−38.0 [44.6]	−42.5 [43.9]
$L_2MH(C_2H_4)_2^+$	**29**	−38.4 [51.4]	−35.3 [53.3]

[a] The MM contribution (kcal/mol) is given in brackets.

the new olefin−metal−ethyl complexes **24a** and **24b**. A new branched polyethylene can be formed from these complexes via reinsertion of propylene (or polymer possessing an α-olefin) into the M−CH_2CH_3 bond. The reaction takes place from **22a-1** and **22b** via transition states **23a** and **23b**, respectively, as shown in Figure 1. The structure **23a** was confirmed to be a real transition state with one imaginary frequency of 227*i* [526*i*] cm^{-1}. Both **23a** and **23b** are very early transition states, especially for M = Ni, with geometries resembling those of reactants **22a** and **22b**, respectively. The energy barriers are 2.2 [7.3] kcal/mol (Gibbs free energy barrier is 1.2 [5.7] kcal/mol) for **22a-1** → **23a** and 2.3 [7.4] kcal/mol for **22b** → **23b**. In other words, the barrier for insertion of an ethylene molecule into the metal−hydride bond is 3 times smaller for Ni than for Pd. The products formed, $L_2M(C_2H_4)(C_2H_5)^+$ (**24a**) and $L_2M(C_3H_6)(C_2H_5)^+$ (**24b**), are 20.9 [22.5] and 22.4 [23.7] kcal/mol, respectively, lower in energy than the corresponding five-coordinate complexes $L_2M(C_2H_4)_2H^+$ (**22a-1**) and $L_2M(C_3H_6)(C_2H_4)H^+$ (**22b**).

Path G. This path corresponds to insertion of olefin (or polymer chain possessing an α-olefin) to form the ethylene−alkyl complex **26b** (or **8** in Scheme 1), which was examined during the discussions[4−6] of path **A**. The structure **25b**, shown in Figure 1, again is a very early transition state, especially for M = Ni. The barrier height is 2.2 [7.6] kcal/mol. The product, **26b** in Figure 1, is 17.4 [19.1] kcal/mol lower in energy than the corresponding five-coordinate species **22b**.

Path H. This corresponds to the rotation of the polymer chain around the M−X axis, X being the center of the an α-olefin C=C bond of the polymer, followed by olefin insertion into the M−H bond, to initiate branched polymer growth. We did not study this path.

IV. Overview of the Chain Transfer/Termination Reactions

Reactions of the Complexes with an Unsubstituted Diimine Ligand (L_2 = [HN=C(H)C(H)=NH]). In the present paper and our previous papers,[4−7] we have discussed the following chain transfer/termination processes for the unsubstituted diimine−M(II)-catalyzed ethylene polymerization reaction: dissociative displacement from olefin−hydride complex **21**, associative displacement and H-exchange, both from the five-coordinate bis(olefin)−hydride complex **22**, and hydrogenolysis.

As discussed in our earlier papers,[4−7] the *β*-hydride transfer/dissociative displacement, path **C**, which starts from the metal−olefin−hydride complex **21** and leads to transfer/termination of the polymer chain through the dissociation of the polymer (propylene in our case), is unlikely to be a favorable chain termination mechanism because the dissociation of propylene is endothermic by about 38 [36] kcal/mol in the gas phase for M = Ni [Pd]. In solution, solvation would make this process much less endothermic. However, this process cannot compete with chain propagation leading to methyl-branched polymers, path **B**, which also starts from the same metal-olefin-hydride complex **21** and is exothermic for reinsertion.

As shown above, the associative displacement mechanism, path **E**, starts from the five-coordinate bis(olefin)−metal−hydride complex **22b** and is also endothermic. However, dissociation of propylene from $L_2M(C_3H_6)(C_2H_4)H^+$ is predicted to be only 12.2 [8.1] kcal/mol endothermic for M = Ni [Pd] in the gas phase, which is much less than the corresponding values for the *β*-hydride transfer/dissociative displacement process. The associative displacement mechanism has to compete with other processes starting from the same five-coordinate complex **22b**: (a) the dissociation of the ethylene molecule (reverse path **D**), which is 7.8 [4.3] kcal/mol endothermic, (b) the H-exchange reaction (path **F**), which takes place with a 2.3 [7.4] kcal/mol barrier, and (c) the reinsertion of propylene (or olefinic polymer) into the M−H bond (path **G**), with a 2.2 [7.6] kcal/mol barrier. For M = Ni, the associative displacement mechanism requires a 12.2 kcal/mol dissociation energy and is not likely to take place, as it cannot compete with paths **F** and **G**, which have only 2.2−2.3 kcal/mol activation barriers and are exothermic. However, for M = Pd, the probabilities of paths **E**−**G** are close to each other with a slight preference for paths **F** and **G**. Therefore, the associative displacement mechanism for chain transfer/termination is more likely for Pd than for Ni. However, the dissociation of ethylene (reverse path **D**) requires about half of the energy needed for paths **E**−**G** for M = Pd. Therefore, most of the five-coordinate complex **22** is likely to go back to **21** to continue on the linear growth path **A**.

The H-exchange process which leads to the diimine−metal−ethyl−olefin complex may, in general, proceed via two different mechanisms. The first of them was studied in our previous paper[5] for the diimine−Pd complex and occurs via a "metathesis-like" transition

Scheme 2. Proposed Elementary Reactions Starting from the Diimine−Metal−Olefin Complex M(H)(C_2H_4) (21; 12 in Scheme 1)[a]

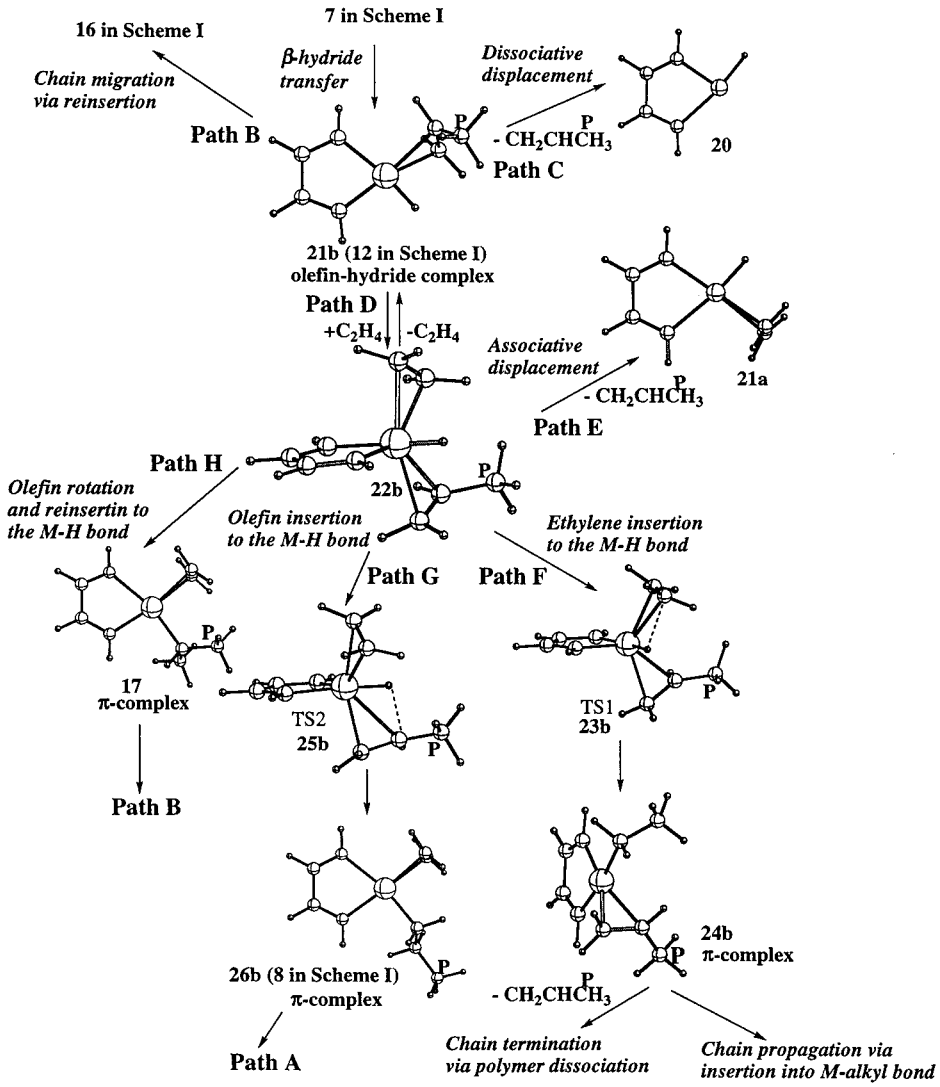

[a] The methyl group labeled "P" is the polymer chain in the polymerization process.

state from **7** without forming a five-coordinate intermediate. This is unlikely to take place because of a high activation barrier of about 40−50 kcal/mol. The second one, studied in the present paper, is a multistep process and includes: (a) oxidative addition of the β-agostic $C^{\beta}-H^{agostic}$ bond to the metal center to form metal−olefin−hydride complex **21**, (b) the coordination of the incoming ethylene molecule to the metal center to form the five-coordinate bis(olefin)−metal−hydride complex **22**, and (c) migration of the hydrogen atom from the metal center to the ethylene molecule. Below we will refer to these mechanisms as "metathesis" and "oxidative addition", respectively. According to our previous[5] and present results, the oxidative addition H-exchange mechanism is the most favorable pathway for chain transfer/termination for both metals. In fact, for the β-agostic-$L_2M(C_3H_7)^+$ complex,[4−6] it was shown that step a takes place with a 14−15 [5−6] kcal/mol barrier and leads to the olefin−hydride complex $L_2M(C_3H_6)H^+$. In the present paper for the $L_2M(C_3H_6)H^+$ complex, we have demonstrated that step b takes place without a barrier and is an exothermic process by 7.8 [4.3] kcal/mol and step c has a 2.3 [7.4] kcal/mol barrier. The entire H-exchange reaction

$$[L_2MCH_2CH_2CH_3]^+ + C_2H_4 \rightarrow [L_2M(H)(CH_2{=}CHCH_3)]^+ + C_2H_4 \rightarrow [L_2M(H)(C_2H_4)(CH_2{=}CHCH_3)]^+ \rightarrow [L_2M(C_2H_5)(CH_2{=}CHCH_3)]^+ \quad (8)$$

is exothermic by 16.7 [22.7] kcal/mol. On the basis of these results, one can conclude that (1) the rate-determining step of the entire oxidative addition H-exchange process is step a for M = Ni and step c for M = Pd, which occur with 14−15 and 7.5 kcal/mol barriers, respectively, (2) the H-exchange chain termination mechanism is the most favorable chain termination process for the unsubstituted diimine−M-catalyzed ethylene polymerization reaction, and (3) it occurs more easily for Pd than for Ni.

In our previous papers,[4−6] hydrogenolysis (reaction 5) has been found to be another favorable chain termination process in the presence of the hydrogen gas pressure and will not be reexamined here.

Reactions with a Substituted Diimine Ligand (ArN=C(H)C(H)=NAr; Ar = 2,6-C_6H_3(*i*-Pr)$_2$). In our

previous paper,[7] we have shown that the replacement of the imine hydrogens with the bulky aromatic group Ar = 2,6-C_6H_3(*i*-Pr)$_2$ decreases the ethylene coordination energy to the transition-metal center and as a result lowers the rate-determining ethylene insertion barrier. These changes are more significant for M = Ni than for M = Pd. The replacement also stabilizes the olefin−hydride complex **12** (or **21**) relative to the *n*-propyl *β*-agostic species **7**, decreases the energy difference between the two, and makes the *β*-H transfer process, leading from the *n*-propyl *β*-agostic species **7** to the olefin hydride intermediate **12** and then to the isopropyl *β*-agostic complex **17**, the most likely mechanism for branching of polyethylenes for the Pd complexes. These results suggest that branching is even more likely in the substituted case. The replacement also increases the propylene dissociation energy from the olefin−hydride complex **12** by 5.1 [1.7] kcal/mol for M = Ni [Pd] and makes the *β*-hydride transfer/dissociative displacement chain termination process less favorable.

As seen from Figure 2 and Table 1, the inclusion of steric effects by the substitution of the imine hydrogens with the bulky aromatic group Ar = 2,6-C_6H_3(*i*-Pr)$_2$ destabilizes the five-coordinate complex **29** and makes it thermodynamically unstable relative to dissociation to C_2H_4 + diimine−$MH(C_2H_4)^+$ (**28**). Therefore, all processes involving the five-coordinate bis(olefin)−metal−hydride complex, paths **D**−**H**, become unimportant. This destabilization is not unexpected, since coordination with the bulky substituents to the crowded metal of five ligands creates additional steric interactions. In fact, according to our IMOMM calculations, the five-coordinate complex **29** lies 0.4 kcal/mol lower [7.2 kcal/mol higher] than the $L_2M(C_2H_4)H^+ + C_2H_4$ dissociation limit for M = Ni [Pd]. The structure of **29** was optimized as a local minimum even for M = Ni in Figure 2, and the reason ethylene does not dissociate must be due to a small barrier between **28** and **29**, which we did not calculate.

Since the five-coordinate bis(olefin)−metal−hydride complex is unstable, the oxidative addition H-exchange chain termination process is unlikely for the substituted-diimine−M(II)-catalyzed polymerization. The other H-exchange chain termination process, via the metathesis mechanism, is unlikely due to the large energetic barrier discussed above. Experimentally, the bulky ligands are required for polymerization to proceed, and this is consistent with the present conclusion that chain transfer/termination via the five-coordinate species is more difficult for substituted diimine catalysts.

V. Comparison of Our Results with Those of Deng, Margl, and Ziegler (DMZ)

We[4,6] and DMZ[9] have published similar papers on the mechanism of the reactions (1), (2), (4), (6), and (7) for the unsubstituted diimine−Ni(II) complexes. In this section, we will compare our results with those of DMZ.

In general, although our results and DMZ's[9a] for polymer initiation reaction 1 are in qualitative agreement, there exist large differences quantitatively. In comparison to the B3LYP method in our paper, the BP86 method used by DMZ shifts the entire potential energy surface (except for the reactant) down by 7−8 kcal/mol. Thus, the barrier from the *π*-complex is nearly

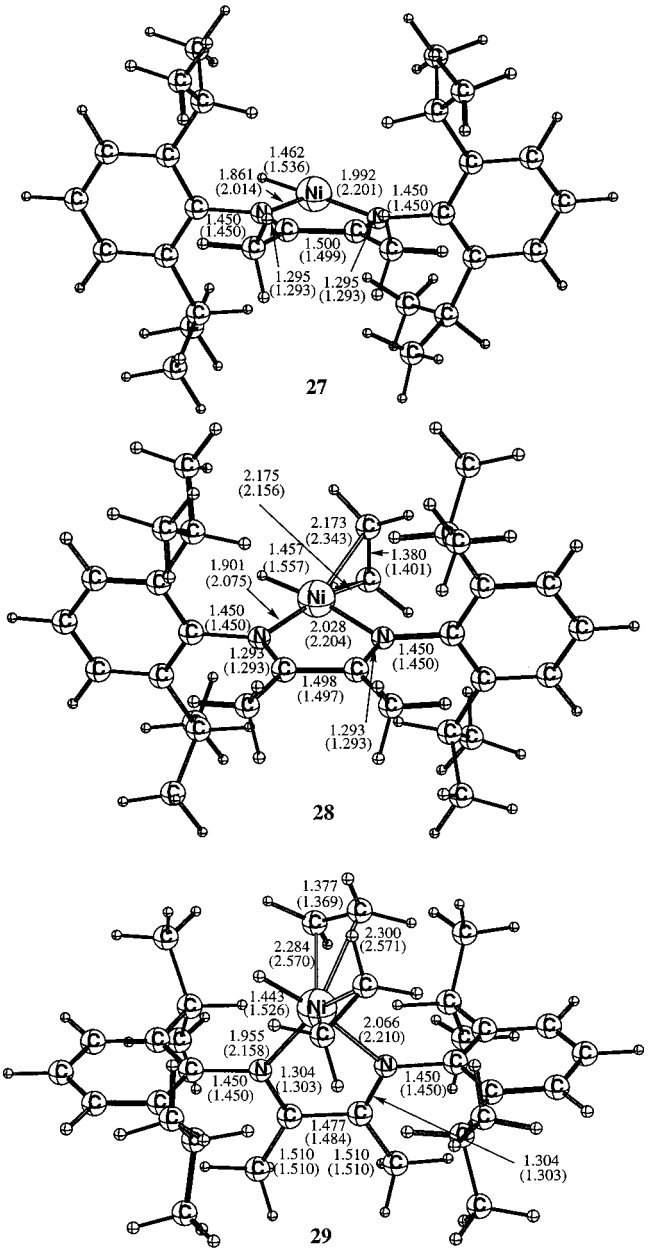

Figure 2. IMOMM(B3LYP/BSI:MM3) optimized structures (bond distances in Å) of L_2MH^+, $L_2MH(C_2H_4)^+$, and $L_2MH(C_2H_4)_2^+$ complexes for M = Ni and Pd (in parentheses) and L_2 = [ArN=C(CH_3)C(CH_3)=NAr], where Ar = 2,6-C_6H_3(*i*-Pr)$_2$.

unchanged, 11.1 kcal/mol vs 9.9 kcal/mol by us, but the exothermicity of the entire reaction (1) increases by 7.6 kcal/mol: 46.9 kcal/mol vs 39.3 kcal/mol by us. These discrepancies in the energetics can be explained in terms of the well-documented trend[11a,l] that the metal−ligand interaction energy by the BP86 method is larger than that with the B3LYP. For instance, the Co−BH_2 {Rh−BH_2 in braces} binding energy with the BP86 method is 76.7 {88.1} kcal/mol, to be compared with 57.2 {81.8} kcal/mol with B3LYP, while the MR−SDCI-(DC)[11a] result, 51.0 {74.1} kcal/mol, is closer to that of B3LYP. The Ni−C_2H_4 bonding energy with BP86 (45.8 kcal/mol) is larger than that with B3LYP (38.9 kcal/mol) and is closer to that with CASPT2 (48.1 kcal/mol).[11l]

For the chain propagation reaction (2) (path **A**) two results are also qualitatively similar, with the following differences.

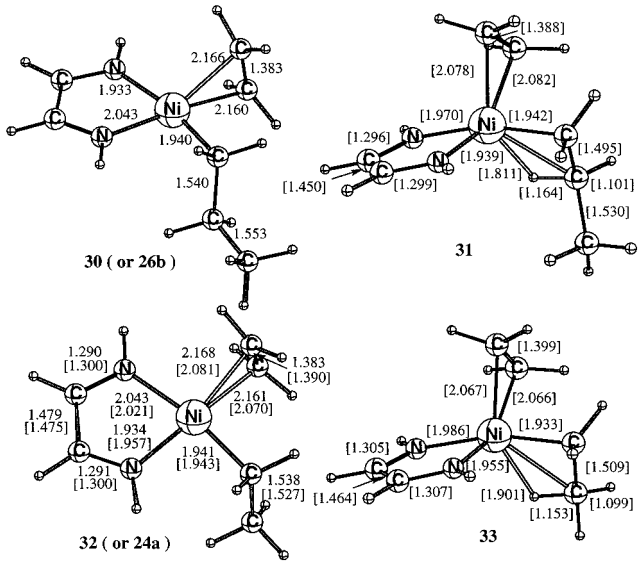

Figure 3. Optimized structures (bond distances in Å) of different possible structures of the complexes $L_2Ni(C_2H_4)(C_3H_7)^+$ and $L_2Ni(C_2H_4)(C_3H_5)^+$ calculated at the B3LYP/BSI and BP86 (in brackets) levels. Structure **31** has been provided by Ziegler et al.[9a]

(I) According to DMZ,[9a] the insertion barrier of the ethylene molecule into the Ni−propyl bond (reaction 2) is 16.8 kcal/mol, which is 5.7 kcal/mol larger than that for the polymer initiation (11.1 kcal/mol; reaction 1) and 6.3 kcal/mol larger than our value of 10.5 kcal/mol. In other words, in our calculations insertion barriers for initiation (with a methyl ligand) and propagation (with *n*-propyl ligand) reactions are about the same, 9.9 and 10.5 kcal/mol, while in DMZ they differ by 5.7 kcal/mol. Note that the experimentally estimated barriers[3a] for the diimine−Pd(II) catalyst, 17.2 and 17.6 kcal/mol for the polymer initiation and polymer propagation reactions, respectively, are also the same and are in excellent agreement with our results,[5] 16.3 and 17.5 kcal/mol, respectively. This difference between our results and those of DMZ[9a] in the calculated barrier heights of the reaction (2) for M = Ni is caused by the difference in the energy of the metal−propyl−ethylene π-complex, the species relative to which the barriers are calculated. Indeed, according to our calculations, the energetically most favorable conformer of the Ni−propyl−ethylene π-complex is the structure **30**, shown in Figure 3, with perpendicular ethylene with respect to the Ni(N═CC═N) plane and without a β-agostic interaction. According to DMZ,[9a] the "trigonal bipyramidal" Ni−propyl−ethylene complex **31**, where the β-agostic interaction is not broken but is weakened by competing for electron density with the ethylene moiety, is energetically lower by 6.5 kcal/mol than **30**.

We have reoptimized the geometries of the diimine−$Ni(C_3H_7)(C_2H_4)^+$ π-complex at the B3LYP/BSI level used throughout this paper. Our optimization procedure, which was performed without symmetry constraints and started from the structure[26] of **31**, converged into structure **30**. This result indicates that at the B3LYP/BSI level **31** obtained by DMZ[9a] is not a minimum on the potential energy surface and the only minimum at this level of theory is **30**. Since the calculations of the diimine−$Ni(C_3H_7)(C_2H_4)^+$ complex are time-consuming, we have performed additional calculations on structures **32** and **33** of the diimine−$Ni(C_2H_5)(C_2H_4)^+$ complex in order to elucidate the role of the methods and basis sets used. The calculated geometries and energetics of these structures are shown in Figure 3 and Table 2, respectively.

(26) The structure provied by Prof. T. Ziegler and Dr. L. Deng.

Table 2. Total Energy (in Hartrees) of Structure 32 of the $L_2M(C_2H_5)(C_2H_4)^+$ (L_2 = [HN═C(H)C(H)═NH]) Complex, the Relative Energy (Relative to 32, in kcal/mol) of Structure 33, and the Ethylene Binding Energy ΔE (in kcal/mol) in 32, Calculated at Various Levels of Theory

method/basis set[a]	π-complex structure **32**	π-complex structure **33**	C_2H_4 binding energy ΔE
BP86/BSI//BP86/BSI	−514.106 791	−0.5	17.6
BP86/BSII//BP86/BSII	−1854.288 286	−1.0	17.0
B3LYP/BSI//B3LYP/BSI	−513.987 524	*b*	12.7
B3LYP/BSII//B3LYP/BSII	−1854.062 826	*b*	12.2
B3LYP/BSI//BP86/BSI	−513.984 778	+2.5	
B3LYP/BSII//BP86/BSII	−1854.059 561	+3.3	

[a] The method and basis set before // are for energy calculations, while those after // are for geometry optimization. BSI is the standard lanl2dz basis set, and BSII is a triple-ζ plus polarization all-electron basis set (see text for more detail). [b] This structure does not exist at the given level of theory and converges into structure **32**.

At first, we used the B3LYP/BSI method. Our optimization was performed without symmetry constraints and started from a structure[26] similar to **33**, and it converged into structure **32**. This result indicates that, at the B3LYP/BSI level, structure **33** does not exist, which is consistent with the aforementioned results for the diimine−$Ni(C_3H_7)(C_2H_4)^+$ complex.

Second, we performed the geometry optimization of structures **32** and **33** at the BP86/BSI level (again without symmetry constraints) and were able to find both minima, among which the structure **33** is 0.5 kcal/mol lower in energy. This result qualitatively agrees with DMZ, while the energy difference between the structures **32** and **33** calculated in this paper, 0.5 kcal/mol, is several times smaller than that obtained by DMZ, 6.5 kcal/mol. A comparison of these results with those obtained at the B3LYP/BSI level shows that the existence of structure **33** on the potential energy surface is the result of using the BP86 density functional.

Third, since DMZ in their calculations[9a] used a triple-ζ-quality basis set including polarization functions on all atoms, we have performed the B3LYP and BP86 calculations with the large basis set II (BSII) described in section II. This basis set includes the all-electron triple-ζ plus polarization set on all active atoms, including Ni, and the 6-31G(d,p) set on the diimine portion. The results quantitatively agree with those obtained using the smaller basis set lanl2dz + 3-21g (BSI). Indeed, at the B3LYP/BSII level, the structure **33** does not exist and converged to the structure **32**. At the BP86/BSII level, both structures exist, and structure **33** is only 1.0 kcal/mol lower than structure **32**. In other words, increasing the basis sets did not change our conclusions regarding the existence of structure **33** and the results of the calculations of DMZ[9a] are due to the BP86 functional.

In Table 2, we also have presented relative energies calculated at the B3LYP level with different basis sets

at the BP86-optimized geometries. A comparison of the energy differences between the structures **32** and **33** obtained at the BP86/BSI and B3LYP/BSI levels, −0.5 and 2.5 kcal/mol, as well as at the BP86/BSII//BP86/BSII and B3LYP/BSII//BP86/BSII levels (the method before // stands for energetics and that after // for geometries), −1.0 and 3.3 kcal/mol, respectively, shows that the BP86 method overstabilizes structure **33**. The "BP86 stabilization" increases only slightly upon enlarging the basis set.

Note that the calculated diimine−$Ni(C_2H_5)^+$ + C_2H_4 complexation energies are 17.6 and 17.0 kcal/mol at the BP86 level and 12.7 and 12.2 kcal/mol at the B3LYP level using basis sets I and II, respectively. In other words, (a) the BP86 method gives a greater coordination energy of ethylene to diimine−$Ni(C_2H_5)^+$ by about 7 kcal/mol, which is consistent with the discussions above and the results from the literature,[11a] and (b) the calculated results are not basis set dependent, as the smaller BSI and the larger BSII provide almost the same results.

(II) A second difference between our studies and those of DMZ[9a] is in the chain propagation reactions 2 and 3. At first, we have found that reaction 2 is exothermic by 63.8 kcal/mol, while DMZ reported 73.0 kcal/mol. We believe again that this difference is the result of the BP86 method used by DMZ, which usually gives stronger metal−ligand interactions, discussed above.

Second, a comparison of the chain isomerization reaction (the beginning of reaction 3) shows that DMZ have failed to locate the olefin−hydride complex diimine−$Ni(CH_2CHCH_3)H^+$. We have located this minimum on the potential energy surface, which lies 13.6 kcal/mol higher than the β-agostic reactant, separated from the latter by a very tight barrier which we could not locate. As was mentioned above, this olefin−hydride complex plays an important role in the associative displacement and/or the H-exchange chain transfer/termination mechanisms, which take place via the five-coordinate bis(olefin)−metal−hydride complex.

The five-coordinate bis(olefin)−metal−hydride complex was successfully located by us and DMZ. In this paper, we have analyzed all of the potential processes initiated from the five-coordinate bis(olefin)−metal−hydride complex in detail for both M = Ni and Pd. However, DMZ discussed the five-coordinate bis(olefin)−metal−hydride complex only in terms of the H-exchange chain termination mechanism for the diimine−Ni complex. The two results again are qualitatively similar, with the following quantitative differences. According to DMZ, the five-coordinate bis(olefin)−metal−hydride complex lies 10.9 kcal/mol lower than the reactants, the β-agostic complex + C_2H_4. However, we have found that it is 3.4 kcal/mol higher than the reactants. This difference is once again related to the fact that the BP86 method used by DMZ gives a stronger metal−ligand interaction than does the present B3LYP method.

VI. Conclusions

From the discussions given above, we may draw the following conclusions.

(1) The β-hydride transfer/dissociative displacement (path **C**), which starts from the metastable metal−olefin−hydride complex **21**, is endothermic by approximately 38 [36] kcal/mol for Ni [Pd] to the dissociation of propylene and cannot compete with paths **B** (leading to methyl-branched polyethylenes) and **D** (coordination of the second olefin to the metal center of the metal−olefin−hydride complex), which also start from the same metal−olefin−hydride complex **21** and are exothermic. This path is an unlikely chain transfer/termination process.

(2) Path **D**, which corresponds to the coordination of a second olefin to the metal center of the metal−olefin−hydride complex to give the five-coordinate complex **22**, is found to be exothermic by 10.3 [6.3] and 7.8 [4.3] kcal/mol for $L_2M(C_2H_4)H^+$ and $L_2M(C_3H_6)H^+$, respectively.

(3) The associative displacement mechanism (path **E**) starts from the five-coordinate bis(olefin)−metal−hydride complex **22** and is endothermic to dissociation of propylene from the $L_2M(C_3H_6)(C_2H_4)H^+$ by only 12.2 [8.1] kcal/mol. This mechanism has to compete with other processes also starting from the same five-coordinate complex: (a) the dissociation of the ethylene molecule (path **D**), which is 7.8 [4.3] kcal/mol endothermic, (b) the H-exchange chain termination reaction (path **F**), which takes place with a 2.3 [7.4] kcal/mol barrier, and (c) the reattaching of the hydrogen to the polymer chain (path **G**) with a 2.2 [7.6] kcal/mol barrier. These results show that, for M = Ni, the associative displacement mechanism cannot compete with paths **F** and **G** and is less likely to take place, while for M = Pd, the probabilities of paths **E**−**G** are very close with a slight preference for paths **F** and **G**. Therefore, for the unsubstituted diimine−Pd complex, the probability of chain transfer/termination via an associative displacement mechanism is higher than for the Ni analogue. This conclusion is consistent with experiment.[3]

(4) The H-exchange process is the most favorable chain termination mechanism for both metals and includes (a) oxidative addition of the β-agostic C^{β}−$H^{agostic}$ bond to the metal center to form metal−olefin−hydride complex **21**, (b) the coordination of the incoming ethylene molecule to the metal center to form the five-coordinate bis(olefin)−metal−hydride complex **22**, and (c) migration of the hydrogen atom from the metal center to the ethylene molecule. Step a, which takes places with a 14−15 kcal/mol barrier, is the rate-determining step for the diimine−Ni-catalyzed process. For the diimine−Pd-catalyzed reaction, step c, which takes place with a 7.4 kcal/mol barrier, is rate-determining.

(5) The substitution of the imine hydrogens with the bulky aromatic group Ar = 2,6-$C_6H_3(i\text{-}Pr)_2$ destabilizes the five-coordinate bis(olefin)−metal−hydride complex and makes it thermodynamically unstable relative to dissociation to C_2H_4 + diimine−$M(C_3H_7)^+$. Therefore, all processes starting from the five-coordinate bis(olefin)−metal−hydride complex become chemically unimportant. The only valid H-exchange chain transfer/termination process is the metathesis mechanism, which probably competes with the β-hydrogen transfer mechanism.

Acknowledgment. We are grateful to Prof. Tom Ziegler and Dr. L. Deng for providing some optimized geometries and for constructive discussions. The use of the computational facilities and programs at the Em-

erson Center for Scientific Computation is acknowledged. The present research is in part supported by a grant (CHE96-27775) from the National Science Foundation. R.D.J.F. acknowledges a Postdoctoral Fellowship from the Natural Sciences and Engineering Research Council of Canada.

OM9711032